Earthq Eng & Eng Vib (2010) 9: 113-122 **DOI**: 10.1007/s11803-010-9059-7

Reduction of structural response to near fault earthquakes by seismic isolation columns and variable friction dampers

Y. Ribakov†

Department of Civil Engineering, Ariel University Center of Samaria, Israel

Abstract: This paper focuses on the investigation of a hybrid seismic isolation system with passive variable friction dampers for protection of structures against near fault earthquakes. The seismic isolation can be implemented by replacing the conventional columns fixed to the foundations by seismic isolating ones. These columns allow horizontal displacement between the superstructure and the foundations and decouple the building from the damaging earthquake motion. As a result, the forces in the structural elements decrease and damage that may be caused to the building by the earthquake significantly decreases. However, this positive effect is achieved on account of displacements occurring in the isolating columns. These displacements become very large when the structure is subjected to a strong earthquake. In this case, impact may occur between the parts of the isolating column yielding their damage or collapse. In order to limit the displacements in the isolating columns, it is proposed to add variable friction dampers. A method for selecting the dampers' properties is proposed. It is carried out using an artificial ground motion record and optimal active control algorithm. Numerical simulation of a seven-story structure shows that the proposed method allows efficient reduction in structural response and limits the displacements at the seismic isolating columns.

Keywords: seismic isolating columns; variable friction dampers; hybrid seismic isolation; near fault earthquakes; control algorithm

1 Introduction

Seismic isolation has been widely used to decouple structures from the impact of damaging earthquakes to reduce the absorption of the earthquake's energy by the superstructure. In some isolators, additional dampers are further supplied to improve the seismic behavior of the superstructure. In isolated structures, displacement is concentrated at the isolators, and the superstructure's inter-story drifts decrease. It was proven that seismic isolation enhances the structures' safety and significantly reduces the design seismic forces (Mayes, 1989). Performance of base isolated buildings during recent earthquakes proved that seismic isolation is an effective alternative to conventional earthquake-resistant design. Laminated rubber bearings and sliding friction pendulums (Al-Hussaini *et al*., 1994) became classic solutions for seismic isolation in thousands of buildings all over the world. A wide review on known base-isolation systems is given by Kelly (1981, 1991), Buckle and Mayes (1990), Zayas *et al*. (1990), Soong and Constantinou (1994), Naeim and Kelly (1999), Stewart *et al*. (1999) and others.

Correspondence to: Y. Ribakov, Department of Civil Engineering, Ariel University Center of Samaria, Israel
Tel. (+972)546-431-385, Fax (+972)390-663-51
E-mail: ribakov@ariel.ac.il
†Senior Lecturer

Received April 7,2009; **Accepted** December 19, 2009

Briman and Ribakov (2006, 2009) studied typical buildings with soft stories in the Mediterranean area. As a rule, these buildings have an RC frame and infill walls at all floors except at the ground floor. The rigidity of the ground floor is much lower than the floors above. It was proposed to use seismic isolating columns (SIC) as alternative devices yielding a similar effect as elastomeric bearings or friction pendulums. The main advantages of the SIC are that they do not require additional space, their lifetime is comparable with that of the structure and no service is required during that period.

As is well-known, the positive effect of seismic isolation is generally achieved on the expanse of big displacements occurring at the isolating devices. These displacements become larger as the magnitude of the earthquake increases. The displacement at the isolator is an especially important parameter for seismic isolating columns, because under a strong earthquake, it may be so big that impact will occur between the parts of the isolating column causing damage or even collapse. Hence, the seismic isolating columns are usually designed for a zone with known seismic activity (Briman and Ribakov, 2009).

A known method for decreasing displacements at the isolators is the addition of supplemental dampers. Passive damping devices are effective in reducing both displacement and base shear for structures that have moderately long periods. Fluid dampers with steel springs that were used with a seismic base isolation system were

discussed by Tezan and Civi (1979). In this case, the spring shifted the natural frequency of the structure and the dampers were used to reduce the amplitudes of the vibrations. However, addition of viscous dampers to base isolators reduces base displacement at the expanse of increasing floor accelerations and inter-story drifts (Kelly, 1999).

Inclusion in base isolation systems of passive friction dampers with constant slip-force is not effective at lower-level earthquakes, because a damped isolation system may be too stiff and so heavily damped that it will not move. To improve the performance of passive dampers, various semi-active dampers were proposed. Barbat *et al*. (1995) studied a hybrid seismic control system combining a class of passive nonlinear base isolator with an active control system. In such a structure-base-isolator system, significant reduction in the absolute base displacement was achieved, but a slight increase in the response of the structure was reported.

Gluck *et al*. (2000) proposed to add a variable stiffness damper to a base isolation system and developed a selective control approach and applied the optimal control forces just when the displacement at the isolators exceeded a certain threshold value. It yielded essential improvement in structural response and saved the energy required for activation of the dampers. Narasimhan and Nagarajaiah proposed a short time Fourier transformation control algorithm for reducing the response of base isolated buildings with variable stiffness isolation systems in near fault earthquakes. It was shown that the controller was effective in reducing the base displacements and interstory drifts without increasing floor accelerations.

Ribakov and Gluck (2002), Loh *et al*. (2003), Choi *et al*. (2008) investigated the application of a semi-active control method utilizing a magnetorheological (MR) damper to reduce the response of an isolated structure subjected to earthquake excitations. Selective and fuzzy-logic control algorithms were applied for calculating the damping required forces. Results of numerical simulations indicated that the proposed algorithms were useful in reducing the seismic response of base-isolated structures.

Ruangrassamee *et al*. (2006) proposed a viscous-plus-variable-friction damping force algorithm, to combine advantageous features of typical viscous and friction dampers, in which the damping force was realized by a MR damper. It was found that with this algorithm, a good accuracy at the excitation frequency of 1 Hz could be achieved. It was also shown that with the use of the damping force algorithm, the base displacement could be reduced by 20%–50%; however, the floor acceleration increased by 20% under some recorded ground motions.

Wongprasert and Symans (2005) experimentally studied a model of a steel frame with a base isolation system consisting of laminated rubber bearings and variable-orifice fluid dampers. The dynamic behavior of the dampers was modulated in accordance with an H_∞ optimal feedback control algorithm. The test results demonstrated that the adaptive isolation system could significantly reduce the superstructure response compared to a conventional passive isolation system.

Lin *et al*. (2007) carried out large-scale experimental tests on a mass equipped with a base-isolation system consisting of rubber bearings and a magnetorheological damper. Various types of passive and semi-active control strategies were compared. It was shown that a combination of rubber bearings and MR dampers could provide robust control of vibration for large civil engineering structures.

Nagarajaiah and Sahasrabudhe (2006) analytically and experimentally investigated the effectiveness of a new semi-active independently variable stiffness device under near fault earthquakes. They developed an average nonlinear tangential stiffness control algorithm for control of the device. It was shown that the device could vary stiffness continuously and smoothly between minimum and maximum stiffness, thus reducing bearing displacements, while maintaining isolation level forces and superstructure responses at the same level as the passive minimum stiffness case.

Casciati *et al*. (2007) introduced a base isolation device consisting of two disks, one vertical cylinder with an upper enlargement sustained by three horizontal cantilevers, and at least three inclined shape memory alloy (SMA) bars. The SMA bars limit the displacement between the base and the superstructure, dissipate energy and guarantee the re-centering of the device. A model of the device was tested on shaking table. It was shown that for cyclic loading, the super-elastic behavior of the alloy results in wide load-displacement loops, where a large amount of energy is dissipated.

Lu *et al*. (2008) studied a sliding base isolation system with controllable stiffness. They proposed to use a semi-active control method developed based on active feedback control to vary the stiffness of the isolation system. It was reported that the proposed system was able to reduce the base displacement and the acceleration of the isolated structure simultaneously.

As mentioned above, recent studies have indicated the high efficiency of hybrid isolation systems. It is evident that applying a control force to the isolation system is required mainly when the displacement at the isolator exceeds a certain threshold value, but for small displacements at the isolator, no control force is needed. Based on this requirement, the current paper focuses on investigating the efficiency of passive variable friction dampers (Ribakov *et al*., 2006) for reduction of displacements in seismic isolating columns.

2 Description of the seismic isolating columns

The seismic isolation column (Briman and Ribakov, 2009) is based on a friction pendulum principle. The

isolator consists of two V-shape elements (A and B), connected to each other by a tie (C) as shown in Fig. 1. The tie is attached to the column at the narrow ends (D and E). The V-shape elements are located one into another with a plane turning of one of them by 90 degrees relative to another one around the vertical axis. The elements have equal height, that is, about 10–15 mm shorter than the entire height of the isolator. It allows mutual horizontal displacements between the elements. A more detailed description of the seismic isolation column, its construction, properties and installation was given by Briman and Ribakov (2009).

A ship chain is attached between the V-shaped elements of the isolator to achieve a pendulum effect. Using ship chains has the advantage that the design load for a standard ship chain is enough for getting the vertical load carried by a single column. Additionally, the internal radius of the curvature of a chain link is very close to the chain cross section radius. Hence sliding friction between the links yields effective energy dissipation.

The connection joint of the tie to the V-shape elements carries all vertical and horizontal loads, allows rotations around any horizontal and vertical axis crossing the joint, and represents a zone where energy dissipation mainly occurs. The isolator has no disadvantages related to technical implementation of the ball and socket connections, i.e., no manufacturing difficulties due to high accuracy requirements, special materials for providing load carrying capacity for all vertical and horizontal forces, etc.

According to Mayes (1989), the natural vibration period of a building with seismic isolation, T_{1-1}, should satisfy the following condition: $T_{1-1} > 5T_1 > 1.5...2.25\,\mathrm{s}$, where T_1 is the dominant natural vibration period of a fixed-based structure. Additionally, damping in an isolated structure should be between 20% and 30%. Following these requirements, parameters of SIC can be determined. The main parameters defining the SIC properties are: the length of the suspension bracket, the radius of the hinges, and the internal space required for free displacements (Briman and Ribakov, 2009).

Practically speaking, buildings with such isolators are designed for an earthquake with a certain peak ground acceleration (PGA). Under a stronger earthquake, the displacement between the V-shaped elements may exceed the designed peak value and it may yield an impact between the V-shaped elements and cause damage to the isolator. This undesired impact would be avoided if, in addition to the isolating columns, the structure is incorporated with dampers.

Note that the maximum permitted horizontal displacement of the base isolator depends on the section dimensions and geometry of the V-shaped elements and should be calculated taking into account real dimensions in each individual case. For example, for a column with a vertical load capacity of 1000 kN, designed for a seismic zone with PGA of 0.2 g, soil type coefficient of 1.2 and near-field coefficient of 1.0, the outside size of the isolation column is about 90 cm and the maximum horizontal displacement, for which impact between the parts of the isolator is prevented, is up to 20 cm (Briman and Ribakov, 2009).

3 Description of the variable friction damper and its properties

A passive variable friction damper (VFD) was proposed by Ribakov *et al*. (2005, 2006). The main distinction of this damper from others is that it uses a wedge-form part, aimed to change the friction force as a function of the displacement transferred to the damper. An additional advantage of this damper is a possibility to design it such that a centering capacity would be provided.

A schematic view of the VFD is shown in Fig. 2. The damper consists of a square section tube (1), a double-wedge (2), two elastic strip elements (3) and a bolted connection clip (4). The wedge is located partially inside the tube and can move ahead and back along its axis. The strips have a cantilever static scheme and are fixed on the tube by the connection clip, forming an elastic strip system. The stiffness of this system may be regulated by changing the location of the connection clip along the tube. The free ends of the cantilever strips have a contact

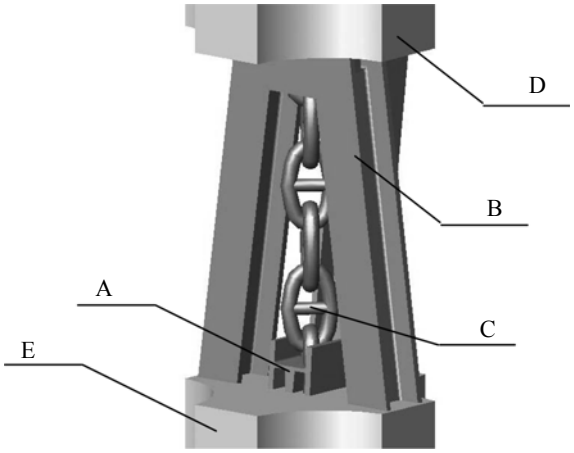

Fig. 1 Internal view of the isolator (following Briman and Ribakov, 2009)

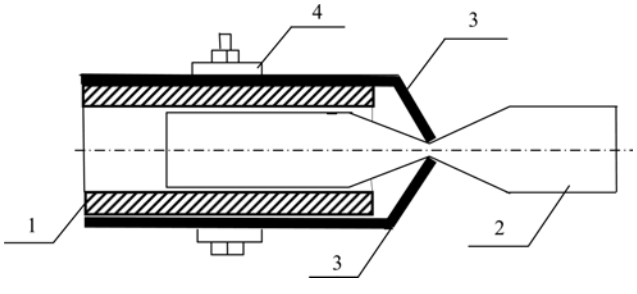

Fig. 2 Schematic view of the VFD (following Ribakov *et al*., 2006)

with an inclined surface of the wedge.

The damper can be attached at the soft floor level as follows. The wedge can be connected through a brace to the foundation, and the tube - to the slab of the isolated superstructure as shown in Fig. 6(b). Alternative connection schemes can also be used. When an earthquake affects the building, the superstructure starts to move relative to the foundation, the displacement at the isolated floor is transferred to the damper and friction forces are developed.

The influence of the wedge inclination angle and the elastic strips flexibility was investigated experimentally and analytically by Ribakov *et al*. (2005, 2006). The experimental results were in a good agreement with those predicted by a theoretical model. It was shown that the damping force, depending on the friction between the wedge and the elastic strip elements and the wedge geometry, can be expressed as follows (Fig. 3):

$$F_D = 2R(\sin\alpha + f\,\mathrm{sign}(x')\cos\alpha) \tag{1}$$

where R is the reaction of the elastic strip element, f is the friction coefficient, α is the wedge inclination angle, and x' is the velocity of the wedge. Defining $F = R f$ and $\rho = \arctan f$, where ρ and f are the friction angle and the friction coefficient, respectively

$$f = \tan\rho \tag{2}$$

Equation (1) can be rewritten as follows:

$$F_D = 2R(\sin\alpha\cos\rho + \mathrm{sign}(x')\cos\alpha\sin\rho)/\cos\rho = 2R\sin(\alpha + \mathrm{sign}(x')\rho)/\cos\rho \tag{3}$$

The reaction of the elastic strip element

$$R = (F_D/2)\cos\rho/\sin(\alpha + \mathrm{sign}(x')\rho) \tag{4}$$

Assume a positive wedge displacement and velocity and decompose the forces acting on the elastic strip element (Fig. 3) to X and Y components. For this case, $\mathrm{sign}(x) = 1$ and

$$X = R(\sin\alpha + f\cos\alpha);\quad Y = R(\cos\alpha - f\sin\alpha) \tag{5}$$

Using simple trigonometric perturbations and substituting f from Eq. (2), yields

$$X = R(\sin\alpha\cos\rho + \cos\alpha\sin\rho)/\cos\rho = R\sin(\alpha+\rho)/\cos\rho = F_D/2 \tag{6}$$

$$Y = R(\cos\alpha\cos\rho - \sin\alpha\sin\rho)/\cos\rho = R\cos(\alpha+\rho)/\cos\rho = (F_D/2)\cot(\alpha+\rho) \tag{7}$$

To obtain the displacement of the elastic strip element along the wedge (Fig. 4), let w and v be displacements in X and Y directions, respectively. In this case

$$w = X\delta_{11} + Y\delta_{21} = (F_D/2)[\delta_{21}/\tan(\alpha+\rho) + \delta_{11}] \tag{8}$$

$$v = Y\delta_{22} + X\delta_{21} = (F_D/2)[\delta_{22}/\tan(\alpha+\rho) + \delta_{21}] \tag{9}$$

where $\delta_{ij}(i = 1, 2; j = 1, 2)$ are the flexibility coefficients; 1 and 2 are the horizontal and vertical directions, respectively.

Defining $C_w = \delta_{21}/\tan(\alpha+\rho) + \delta_{11}$ and $C_v = \delta_{22}/\tan(\alpha+\rho) + \delta_{21}$, Equations (8) and (9) obtain the following forms:

$$w = (F_D/2)C_w,\quad v = (F_D/2)C_v \tag{10}$$

The overall vertical displacement of the strip end is

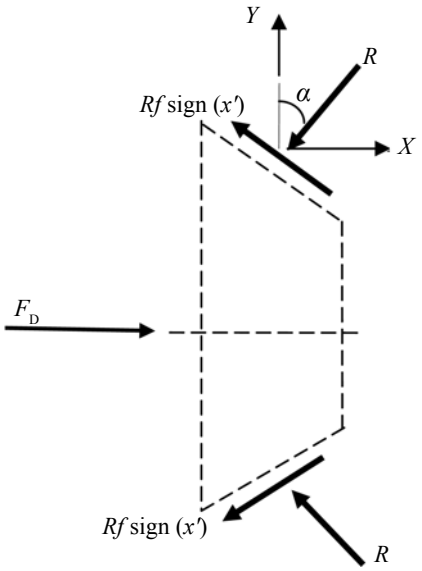

Fig. 3 Forces acting on the elastic strip elements (following Ribakov *et al*., 2006)

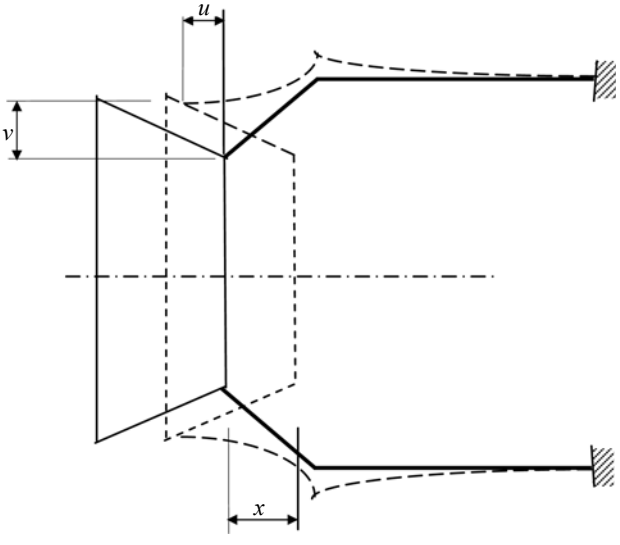

Fig. 4 Displacements calculation scheme (following Ribakov *et al*., 2006)

$$v = (x - w) \tan \alpha \tag{11}$$

Substituting Eq. (10) into Eq. (11) yields:

$$(F_D / 2)\, C_v / \tan \alpha = x - (F_D / 2)\, C_w \tag{12}$$

or

$$(F_D / 2)\, (C_w + C_v / \tan \alpha) = x \tag{13}$$

Hence, the damping force as a function of wedge displacement is:

$$F_D = 2\, x / (C_w + C_v \cot \alpha) \tag{14}$$

As mentioned above, this equation is valid for positive wedge displacement and velocity ($x > 0$, $x' > 0$). However, when the velocity changes its sign, the friction force acts in an opposite direction. Hence the loading and unloading paths are different. A typical force – displacement relationship in a VFD is shown in Fig. 5, where $F_{FR,\,max}$ represents the maximum friction force that is achieved at maximum wedge displacement, $x_{VFD,\,max}$. $F_{D,\,max}$ is the maximum damping force, obtained at maximum displacement in the VFD according to Eq. (14). These three parameters are used for design of the VFD as discussed below.

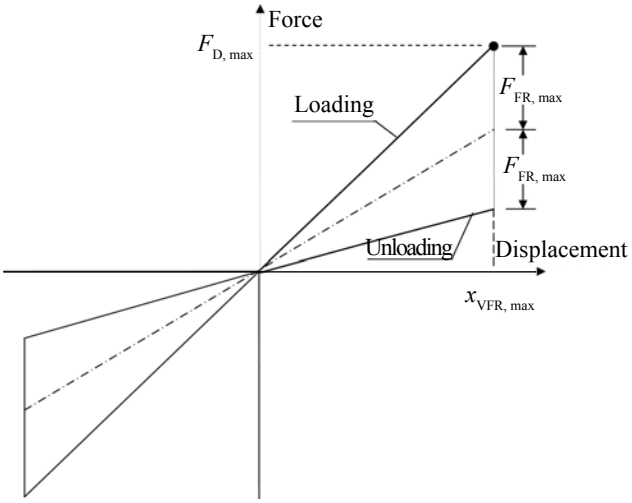

Fig. 5 Relationship between damping forces and displacement in a VFD (following Ribakov *et al*., 2006)

Ribakov *et al*. (2006) demonstrated experimentally that the hysteretic loops area for VFD may be increased almost three times by appropriate changing of the damper's parameters. In this study, a method for selecting the parameters of the VFD aimed at achieving efficient reduction in structural seismic response and decreasing the displacement at the SIC is proposed.

4 Selection of VFD parameters

In selecting the properties of the VFD to be attached to the isolation system to limit the displacement at the SIC within an allowed value, the response of the structure with SIC and active dampers to an artificial white noise earthquake is calculated. The force in the active dampers can be obtained using an optimal active control algorithm. In this study, it was calculated using the instantaneous closed loop control algorithm presented in detail by Soong (1990).

Following this algorithm, the response of a base isolated structure with active dampers can be described by the following dynamic equilibrium equation:

$$\boldsymbol{M}\ddot{\boldsymbol{x}}(t) + \boldsymbol{C}\dot{\boldsymbol{x}}(t) + \boldsymbol{K}\boldsymbol{x}(t) = \boldsymbol{L}\boldsymbol{f}_e(t) + \boldsymbol{D}\boldsymbol{u}_c(t) \tag{15}$$

where $\boldsymbol{M}$, $\boldsymbol{C}$, and $\boldsymbol{K}$ are the mass, the damping, and the stiffness matrices, respectively; $\boldsymbol{x}(t)$, $\dot{\boldsymbol{x}}(t)$, $\ddot{\boldsymbol{x}}(t)$ are the displacement, the velocity and the acceleration vectors, respectively; $\boldsymbol{u}_c$ is the vector of control forces in the supplemental devices; $\boldsymbol{f}_e$ is the external excitation; $\boldsymbol{D}$ and $\boldsymbol{L}$ are the location matrices of the control and excitation forces, respectively.

According to the instantaneous control rules, a time-dependent performance index, $J(t)$, defined by the following equation is introduced

$$J(t) = \boldsymbol{z}^T(t)\boldsymbol{Q}\boldsymbol{z}(t) + \boldsymbol{u}_c^T(t)\boldsymbol{R}\boldsymbol{u}_c(t) \tag{16}$$

where $\boldsymbol{R}$ and $\boldsymbol{Q}$ are weighting matrices which define the priorities between the energies dissipated in the structural elements and in the dampers. In this study, the matrices $\boldsymbol{R}$ and $\boldsymbol{Q}$ are assumed to be

$$\boldsymbol{R} = 10^{-m}\, \boldsymbol{I} \qquad \boldsymbol{Q} = \boldsymbol{I}_{2n \times 2n} \tag{17}$$

where $\boldsymbol{I}$ is a $2n \times 2n$ unit diagonal matrix, and m is a parameter which keeps the damping forces within the dampers' practical capacity. This parameter is selected so that the displacement at the SIC would remain within the allowed limit.

This second order differential equation (Eq.(15)) may be transformed into the space state form as follows:

$$\dot{\boldsymbol{z}}(t) = \boldsymbol{A}\boldsymbol{z}(t) + \boldsymbol{B}\boldsymbol{u}_c(t) + \boldsymbol{H}\boldsymbol{f}_e(t) \tag{18}$$

where $\boldsymbol{z}(t) = [\boldsymbol{x}(t), \dot{\boldsymbol{x}}(t)]^T$ is the 2 n space state vector of the displacements and velocities for each of the n DOFs of the structure, $\boldsymbol{A}$ is the system's matrix, $\boldsymbol{B}$ defines the control location, and $\boldsymbol{H}$ is the excitation forces location matrix:

$$\boldsymbol{A} = \begin{bmatrix} \boldsymbol{0} & \boldsymbol{I} \\ -\boldsymbol{M}^{-1}\boldsymbol{K} & -\boldsymbol{M}^{-1}\boldsymbol{C} \end{bmatrix}, \quad \boldsymbol{B} = \begin{bmatrix} \boldsymbol{0} \\ \boldsymbol{M}^{-1}\boldsymbol{D} \end{bmatrix},$$

$$\boldsymbol{H} = \begin{bmatrix} \boldsymbol{0} \\ \boldsymbol{M}^{-1}\boldsymbol{L} \end{bmatrix} \tag{19}$$

Following Soong (1990), the force in the active dampers

$$\boldsymbol{u}_{\mathrm{c}}(t) = -\frac{\Delta t}{2}\boldsymbol{R}^{-1}\boldsymbol{B}^{\mathrm{T}}\boldsymbol{Q}\,\boldsymbol{z}(t) \tag{20}$$

Analysis of the building's response at discrete time steps to an artificial white noise ground motion yields the optimal forces for each time increment. The VFD attached to the structure will yield similar reductions in the displacements at the SIC if the damping force in the VFD will be as close as possible to the force developed by an optimally controlled active device. However, the force-displacement relationship in VFD is different from active controlled devices. Hence it was assumed in this study that the maximum displacement in the active controlled building equals that of VFD, $x_{\mathrm{VFD,\,max}}$. An additional assumption is that the maximum force that was applied to the isolated structure by the active controlled device should be equal to the maximum damping force, produced by the VFD, $F_{\mathrm{D,\,max}}$. It was further assumed in this study that the parameters of VFD should be selected so that the damping force would be equal to zero on unloading branch (Fig. 5) when the SIC returns to its initial static equilibrium position.

5 Numerical example

5.1 Description of the structure

In order to examine the efficiency of the hybrid seismic isolation system including VFD, a numerical simulation of a seven-story building was carried out. The response of a plane frame with stiff beams shown in Fig. 6 was analyzed. Passive base isolation is known to be a more effective method for low rise buildings and for medium or high rise buildings using dampers, distribution along the height may be recommended. However, recent advances in seismic isolation devices have enabled the base isolation technique to also be applied to high-rise buildings (Nobuyuki *et al*., 2006, Ariga *et al*., 2006). Using seismic isolation columns with VFD yields lower cost and, as demonstrated below, provides the desired effect. All simulations were performed using originally developed routines, written in MATLAB, and using the Control System Toolbox (Control System Toolbox For Use with MATLAB, 1999). An initial damping ratio of 1% was assumed for all vibration modes of the uncontrolled structure.

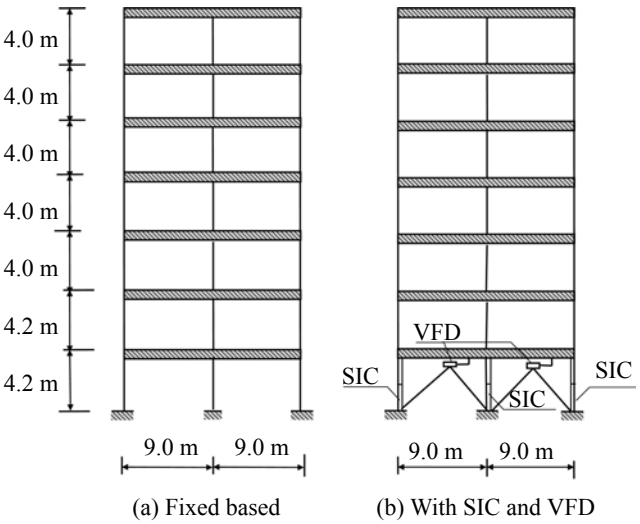

Fig. 6 Seven-story structure

The following matrices characterize the structure:

$$\boldsymbol{M} = 8.75\times10^{4}\,\boldsymbol{I}_{7\times7}\ \text{[kg-mass]}$$

$$\boldsymbol{K} = \begin{bmatrix} 29.28 & -14.64 & & & & & 0 \\ -14.64 & 31.59 & -16.95 & & & & \\ & -16.95 & 30.96 & -14.01 & & & \\ & & -14.01 & 28.02 & -14.01 & & \\ & & & -14.01 & 25.13 & -11.12 & \\ & & & & -11.12 & 22.24 & -11.12 \\ 0 & & & & & -11.12 & 11.12 \end{bmatrix} \times10^{7}\ \text{[N / m]}$$

where $\boldsymbol{M}$ is the mass matrix of the structure, $\boldsymbol{I}_{7\times7}$ is a unit diagonal matrix and $\boldsymbol{K}$ is the structural stiffness matrix. An initial damping ratio of 1% was assumed for all vibration modes of the uncontrolled structure.

In the numerical example, the following cases will be considered and compared:

- Case 1: an uncontrolled fixed-base structure;
- Case 2: a structure with SIC without dampers;
- Case 3: a structure with SIC and active controlled devices;
- Case 4: a structure with SIC and passive VFD.

Following Mayes (1989), the natural vibration period of the isolated structure was assumed to be equal to $5T_1$. The isolating columns were designed for a seismic zone with PGA = 0.2 g and the maximum horizontal displacement at the isolated floor for this case without impact between the parts of the isolation columns is up to 20 cm (Briman and Ribakov, 2009). Hence, the limit value of the displacements in the SIC is assumed to be 20 cm to achieve the desired seismic isolation effect.

For design purposes, in order to exceed this limit, the structure with SIC (cases 2 and 3) was further subjected to an artificial white noise ground motion with a PGA = 0.3 g. Maximum forces in active dampers and appropriate displacements were obtained and the properties of equivalent VFD were selected. Then, response of a structure with VFD (Case 4) to the artificial ground motion and to real earthquakes was compared to that with active devices (Case 3).

5.2 Finding the properties of equivalent VFD using an artificial ground motion

In the first stage, the structural response to a white

noise ground motion with the following properties was calculated for cases 1 and 2: PGA = 0.3g, BW = 10 Hz and t_f = 70 s. The peak displacement at the SIC for case 2 was 41.05 cm, which more than twice exceeds the limit value. For this reason, the response of the structure for Case 2 is not presented as it has no physical meaning.

In the second stage, the response of the isolated structure with active dampers attached at the first floor was obtained. The aim of the control was to reduce the displacements at the SIC below the limit value. Following the results of numerical analysis, the peak control force for this case was 1301.3 kN and the corresponding displacement at the SIC was 6.12 cm.

As mentioned above, in order to achieve similar effects in reducing displacements at the SIC by using passive VFD, it was assumed that the damping force in the VFD, for this displacement value ($x_{VFD,\ max}$ = 6.12 cm) should be equal to the control force, developed by active devices ($F_{D,\ max}$ = 1301.3 kN). In the third stage, the response of the structure with equivalent VFD was obtained. Peak values of floor displacements, displacements at the SIC and peak roof accelerations are presented in Table 1. Time history of roof displacements is shown in Fig. 7. Floor displacements for cases 3 and 4 in the table and in Table 4 are shown relative to the upper SIC end and the peak roof accelerations represent the total values (including the ground acceleration).

As it follows from the table and the figure, the response of the structure with passive VFD is close to that with active devices. Selection of parameters of the VFD using the proposed approach allowed reduction of maximum displacements at the SIC from 8.51 to 6.74 cm. The peak displacements in the structure with equivalent VFD were reduced almost three times compared to the uncontrolled structure. There was no significant difference between the peak roof accelerations of the isolated structure with active controlled devices and that with equivalent VFD. The results, obtained using the artificial ground motion, were further verified using natural earthquake records.

5.3 Structural response to natural earthquake records

The response of the structure to the following near fault earthquakes was simulated: Tabas (1978), Loma-Prieta (1989) and Kobe (1995). Characteristics of these earthquakes are given in Table 2. The peak base displacements in the SIC for Case 2 under the above-mentioned earthquakes were 81.23 cm, 34.41 cm and 84.5 cm, respectively, which exceeds the limit value.

Time histories of the roof displacements for cases 1, 3 and 4 under the natural earthquakes are given in Fig. 8. Tables 3, 4 and 5 present the peak displacements in the structure and peak roof accelerations for the above mentioned study cases under the same earthquakes.

Table 1 Peak displacements in the structure subjected to artificial white noise ground motion

Floor	Displacement (cm)		
	Case 1	Case 3	Case 4
1	2.32	-	-
2	4.51	0.72	0.89
3	6.23	1.39	1.61
4	8.00	2.18	2.37
5	9.38	2.82	2.91
6	10.62	3.39	3.41
7	11.27	3.67	3.71
SIC	-	6.12	6.74
	Acceleration (m/s^2)		
Roof	5.79	1.81	1.95

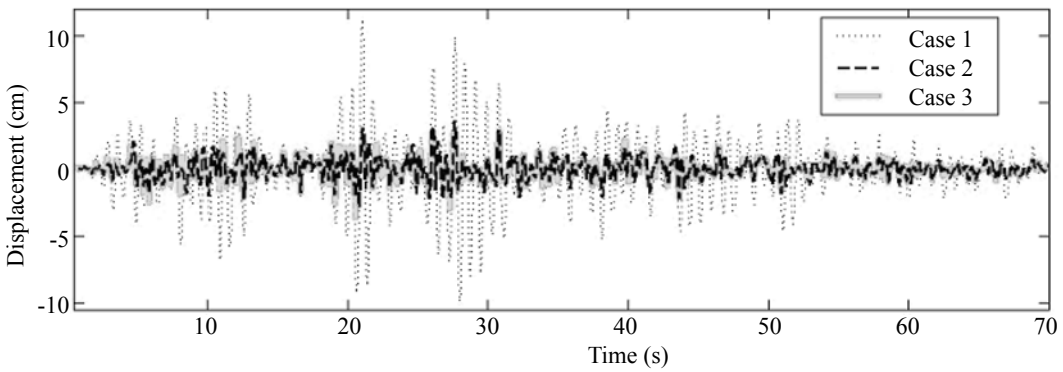

Fig. 7 Roof displacements time history under a white noise ground motion

Table 2 Characteristics of historical ground motions used in this study

Earthquake	Magnitude	PGA (g)	Distance (km)
Tabas (1978)	7.4	0.90	1.2
Loma Prieta (1989)	7.0	0.37	6.3
Kobe (1995)	6.9	1.09	3.4

Table 3 Peak displacements in the structure subjected to Tabas earthquake

Floor	Displacement (cm)		
	Case 1	Case 3	Case 4
1	5.60	-	-
2	10.85	2.08	2.59
3	14.98	3.82	4.31
4	19.31	5.46	6.15
5	22.95	6.83	7.61
6	23.32	7.82	8.95
7	28.15	8.40	9.82
SIC	-	10.18	14.33
	Acceleration (m/s^2)		
Roof	5.25	1.23	1.40

Table 4 Peak displacements in the structure subjected to Loma Prieta earthquake

Floor	Displacement (cm)		
	Case 1	Case 3	Case 4
1	2.57	-	-
2	5.03	0.87	0.94
3	6.95	1.56	1.74
4	8.94	2.26	2.79
5	10.48	2.88	3.67
6	11.75	3.52	4.61
7	12.39	3.84	5.14
SIC	-	7.61	8.51
	Acceleration (m/s^2)		
Roof	4.28	1.44	1.52

Table 5 Peak displacements in the structure subjected to Kobe earthquake

Floor	Displacement (cm)		
	Case 1	Case 3	Case 4
1	12.67	-	-
2	24.42	4.39	4.97
3	33.81	7.79	8.22
4	43.67	11.19	10.61
5	51.57	13.75	12.71
6	58.40	15.99	15.63
7	61.93	17.24	16.77
SIC	-	15.60	19.72
	Acceleration (m/s^2)		
Roof	4.82	1.57	1.69

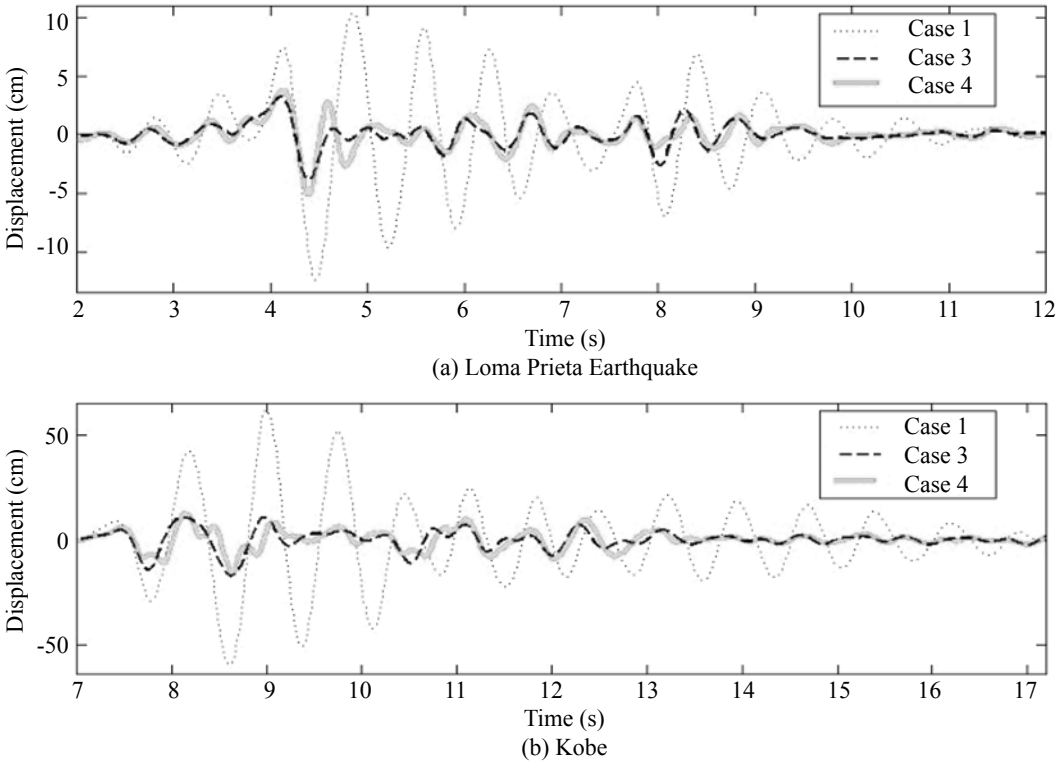

Fig. 8 Roof displacements time history under near fault earthquakes

As in the case of the white noise ground motion, floor displacements for cases 3 and 4 in Tables 3 - 5 and in Fig. 8 are shown relative to the upper SIC end.

Note that the roof displacements in the structure are similar for cases 3 and 4. They are significantly lower than those in a fixed based structure (Case 1). Using VFD selected according to the proposed method (Case 2) yields a significant reduction in peak displacements at the SIC. For all earthquakes that were used for numerical analysis in this study, the peak displacements at the SIC were within the allowed limit. It should be mentioned that even for the Kobe earthquake having a PGA of 1.09 g, the VFD demonstrated high efficiency and yielded significant reduction in structural seismic response. For this earthquake, the system with VFD yielded even higher reduction of the peak roof displacements than that with active controlled devices (see Table 5).

Reductions from 58% to 73% were obtained in peak floor displacements of the isolated structure with VFD (Case 4) compared to the uncontrolled fixed-base one (Case 1). The reduction of peak floor displacements in a structure with optimal active dampers (Case 3) compared to Case 1 was from 69% to 72%. The peak displacements at the SIC for Case 4 were lower by 75% to 82% compared to Case 2. Addition of active controlled devices (Case 3) allowed reduction in peak displacements at the SIC from 78% to 88%. There were no significant differences in the peak values of roof accelerations for Cases 3 and 4. This indicates that the behavior of the isolated structure was almost the same for Cases 3 and 4, demonstrating high efficiency of passive VFD added to SIC.

6 Conclusions

A hybrid seismic isolation system with passive variable friction dampers, aimed to protect structures from strong earthquakes, was studied. The effect of seismic isolation was obtained by replacing the conventional columns fixed to the foundations by seismic isolating ones allowing horizontal displacement between the superstructure and the foundations. The role of dampers is to reduce displacements in the isolation system under strong earthquakes.

A simple method for selecting the dampers' properties was proposed. Properties of variable friction dampers were selected using an artificial ground motion record and optimal active control algorithm. Numerical simulation of a seven-story structure shows that the proposed method allows efficient reduction in structural response and limits the displacements at the seismic isolating columns.

The structure selected for numerical analysis was further submitted to natural near fault earthquakes. It was demonstrated that addition of passive dampers designed according to the proposed method to a seismic isolation system leads to similar behavior as in the case of active devices. The peak floor displacements and peak roof accelerations were significantly reduced compared to a fixed-based uncontrolled structure. The peak displacements in the isolating devices were much lower relative to a structure with an isolating system without dampers. Hence, passive variable friction dampers appear to be very attractive for practical implementations in base isolated buildings designed for near fault earthquakes.

References

Al-Hussaini TM, Zayas VA, Constantinou MC (1994), "Seismic Isolation of Multi-story Frame Structures Using Spherical Sliding Isolation Systems," *Technical Report NCEER 94-0007*, State University of New York at Buffalo, Department of Civil Engineering, Buffalo, NY.

Ariga T, Kanno Y and Takewaki I (2006), "Resonant Behaviour of Base-isolated High-rise Buildings Under Long-period Ground Motions," *The Structural Design of Tall and Special Buildings*, **15**: 325–338.

Barbat AH, Rodellar J, Ryan EP and Molinares N (1995), "Active Control of Nonlinear Base-isolated Buildings," *Journal of Engineering Mechanics*, **121**(6): 676–685.

Briman V and Ribakov Y (2006), "Seismic Isolation Columns for Earthquake-resistant Structures," *The Structural Design of Tall and Special Buildings*, **17**(1): 99–116.

Briman V and Ribakov Y (2009), "Using Seismic Isolation Columns for Retrofitting Buildings with Soft Stories," *The Structural Design of Tall and Special Buildings*, **18**: 507–523.

Buckle IG and Mayes RL (1990), "Seismic Isolation: History, Application, and Performance — a World View," *Earthquake Spectra*, **6**(2): 161–201.

Casciati F, Faravelli L and Hamdaoui K (2007), "Performance of a Base Isolator with Dhape Memory Alloy Bars," *Earthquake Engineering and Engineering Vibration*, **6**(4): 401–408.

Choi KM, Jung HJ, Lee HJ and Cho SW (2008), "Seismic Protection of Base-isolated Building with Nonlinear Isolation System Using Smart Passive Control Strategy," *Structural Control and Health Monitoring,* **15**(5): 785–796.

Control System Toolbox For Use with MATLAB - User's Guide, The MathWorks, Inc., 1999.

Gluck J, Ribakov Y and Dancygier AN (2000), "Selective Control of Base Isolated Structures with CS Dampers," *Earthquake Spectra*, **16**: 593–606.

Kelly JM (1981), "Aseismic Base Isolation: History and Prospects," *Proc. 1st World Congress on Joints and Bearing*s, ACI-SP-70, **1**: 549–586.

Kelly JM (1991), "Base Isolation: Origins and Development," *News – Earthquake Engineering Research Center*, **12**(1): 1–3.

Kelly JM (1999), "The Role of Damping in Seismic Isolation," *Earthquake Engineering and Structural Dynamics,* **28**: 3–20.

Lin PY, Roschke PN and Loh CH (2007), "Hybrid Base-isolation with Magnetorheological Damper and Fuzzy Control," *Structural Control & Health Monitoring*, **14**(3): 384–405.

Loh CH, Wu LY and Lin PY (2003), "Displacement Control of Isolated Structures with Semi-active Control Devices," *Journal of Structural Control*, **10**(2): 77–100.

Lu LY, Lin GL and Kuo TC (2008), "Stiffness Controllable Isolation System for Near-fault Seismic Isolation," *Engineering Structures*, **30**(3): 747–765.

Mayes RL (1989), "Design of Structures with Seismic Isolation," *The Seismic Design Handbook*, New York: Van Nostrand Reinhold, pp. 413–438.

Naeim F and Kelly JM (1999), *Design of Seismic Isolated Structures*, New York: John Wiley & Sons, Inc..

Nagarajaiah S and Sahasrabudhe S (2006), "Seismic Response Control of Smart Sliding Isolated Buildings Using Variable Stiffness Systems: an Experimental and Numerical Study," *Earthquake Engineering and Structural Dynamics*, **35**: 177–197.

Narasimhan S and Nagarajaiah S (2005), "STFT Algorithm for Semiactive Control of Base Isolated Buildings with Variable Stiffness Isolation Systems Subjected to Near Fault Earthquakes," *Engineering Structures*, **27**(4): 514–523.

Nobuyuki O, Hiroyuki A, Yasufumi K and Toshio M (2006), "Design Example of Base-isolated High-rise Building with Large Aspect Ratio," *Kumagai Technical Research Report*, **64**: 53–60.

Ribakov Y, Blostotsky B and Iskhakov I (2005), "Modeling and Design of Variable Friction Dampers for Improving Seismic Response of Structures," *The Tenth International Conference on Civil and Structural Engineering Computing*, Rome, 30 August -02 September 2005, Paper 209.

Ribakov Y, Blostotsky B and Iskhakov I (2006), "Theoretical Model and Laboratory Tests of a Variable Friction Damper," *European Earthquake Engineering*, **20**(1): 43–47.

Ribakov Y and Gluck J, (2002), "Selective Controlled Base Isolation System with Magnetorheological Dampers," *Earthquake Engineering and Structural Dynamics*, **31(**6): 1301–1324.

Ruangrassamee A, Srisamai W and Lukkunaprasit P (2006), "Response Mitigation of the Base Isolated Benchmark Building by Semi-active Control with the Viscous-plus-variable-friction Damping Force Algorithm," *Structural Control and Health Monitoring*, **13**(2-3): 809–822.

Soong TT (1990), *Active Structural Control: Theory and Practice*, NY: John Wiley & Sons, Inc.

Soong TT and Constantinou MC (1994), *Passive and Active Structural Vibration Control in Civil Engineering*, New York: Springer-Verlag.

Stewart JP, Conte JP and Aiken ID (1999), "Observed Behavior of Seismically Isolated Buildings," *Journal of Structural Engineering*, ASCE, **125**(9): 955–964.

Tezan S and Civi A (1979), "Reduction in Earthquake Response of Structures by Means of Vibration Isolation," *Proceedings of the Second U.S. National Conference on Earthquake Engineering*, pp. 433–442.

Wongprasert N and Symans MD (2005), "Experimental Evaluation of Adaptive Elastomeric Base-isolated Structures Using Variable-orifice Fluid Dampers," *Journal of Structural Engineering*, **131**(6): 867–877.

Zayas V, Low S and Mahin S (1990), "A Simple Pendulum Technique for Achieving Seismic Isolation," *Earthquake Spectra*, **6**(2): 317–334.